JOC The Journal of Organic Chemistry

Article

pubs.acs.org/joc

Theoretical Studies of Ring-Opening Reactions of Phenylcyclobutabenzenol and Its Reactions with Alkynes Catalyzed by Rhodium Complexes

Yang Li and Zhenyang Lin*

Department of Chemistry, The Hong Kong University of Science and Technology, Clear Water Bay, Kowloon, Hong Kong, People's Republic of China

Supporting Information

ABSTRACT: DFT calculations have been carried out to study the Rh-catalyzed site selective ring-opening reactions of phenylcyclobutabenzenol (**1a**). Our calculations supported that the mechanism involves β-carbon elimination in a rhodium(I) phenylcyclobutabenzenolato complex followed by alcoholysis. The favorable β-carbon elimination involves the cleavage of the C(sp^2)−C(sp^3)(OH)(Ph) bond in **1a**, which determines the site selectivity. The mechanism and regioselectivity of the related Rh-catalyzed insertion reaction of the asymmetric alkyne MeC≡CPh with phenylcyclobutabenzenol (**1a**) was also investigated. The key step involves the alkyne insertion into the Rh−C σ bond of a species resulting from the favorable β-carbon elimination in the rhodium(I) phenylcyclobutabenzenolato complex. The favorable insertion couples the metal-bonded carbon with the methyl-substituted carbon of MeC≡CPh.

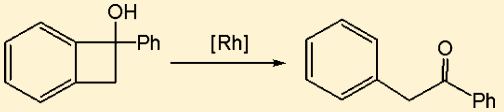

INTRODUCTION

Carbon−carbon single bonds are among the least reactive functional groups in chemistry. As a result, the cleavage of carbon−carbon single bonds is one of the most challenging reactions and attracts considerable attention.[1] Chemically, ring-opening reactions often involve cleavage of carbon−carbon bond(s) and are normally carried out under thermal and/or photochemical conditions.[2] Recent development shows that ring-opening reactions related to cleavage of carbon−carbon bond(s) can also be realized through transition-metal-catalyzed (Pd,[3] Ni,[4] Cu,[5] Zn,[6] Co,[7] and Au[8]) reactions. Despite the fact that the computational chemistry approach has been widely employed to explore reaction mechanisms of various chemical reactions, it is surprising to find that computational studies of carbon−carbon bond cleavage reactions involving ring opening are limited.[9]

In this paper, we are interested in the Rh-catalyzed ring-opening reactions of benzocyclobutenols reported recently by Murakami et al.[10] In the catalyzed reactions, interesting site selectivity in the ring opening was observed. For example, simple heating of phenylcyclobutabenzenol (**1a**) in toluene at 100 °C selectively cleaved the C(sp^3)−C(sp^3) single bond and gave 2-methylbenzophenone (**2a**) in high yield (eq 1). However, when **1a** was heated at 100 °C in toluene in the presence of $[Rh(OH)(cod)]_2$ (2.5 mol %), 1,2-diphenylethanone (**3a**) was exclusively obtained as a result of the cleavage of one C(sp^2)−C(sp^3) single bond (eq 2). The finding of this site selectivity further prompted the same research group to examine reactions of benzocyclobutenols with alkynes under the same catalytic reaction conditions. Equation 3 gives examples of such reactions, showing the successful insertion of alkynes into the C(sp^2)−C(sp^3)(OH)(Ph) single bond of phenylcyclobutabenzenol (**1a**).

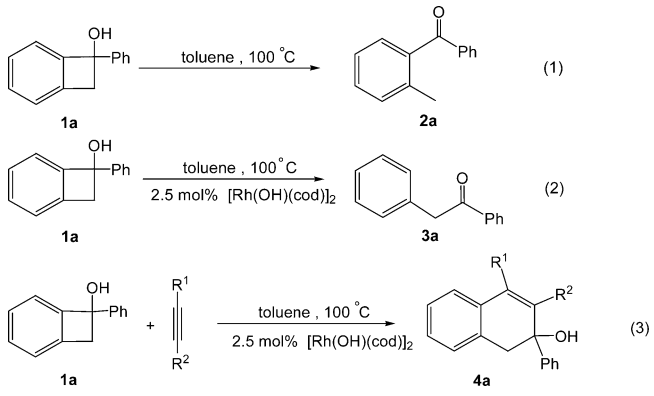

On the basis of their experimental observations related to the site selectivity in the ring-opening reactions, Murakami et al. proposed a mechanism involving β-carbon elimination followed by protonation (alcoholysis) to account for the reactions. Scheme 1 shows the proposed mechanism using phenylcyclobutabenzenol (**1a**) as the substrate and $RhL_2(OH)$ (L_2 = COD) as the precatalyst. **1a** coordinates to the rhodium metal center of the precatalyst followed by deprotonation to give **A**, an active species entering the catalytic cycle. In the active species **A**, the arene moiety from the phenylcyclobutabenzenolate ligand coordinates to the rhodium metal center in an η^2 fashion. From the active species **A**, β-carbon elimination cleaves a C(sp^2)−C(sp^3) single bond of the phenylcyclobutabenzenolate ligand, giving the ring-opened arylrhodium intermediate **BP**. From **BP**, a ligand exchange of a phenylcyclobutabenzenol molecule (**1a**) for the coordinated C═O moiety

Received: August 29, 2013
Published: October 14, 2013

dx.doi.org/10.1021/jo4019123 | J. Org. Chem. 2013, 78, 11357−11365

Scheme 1

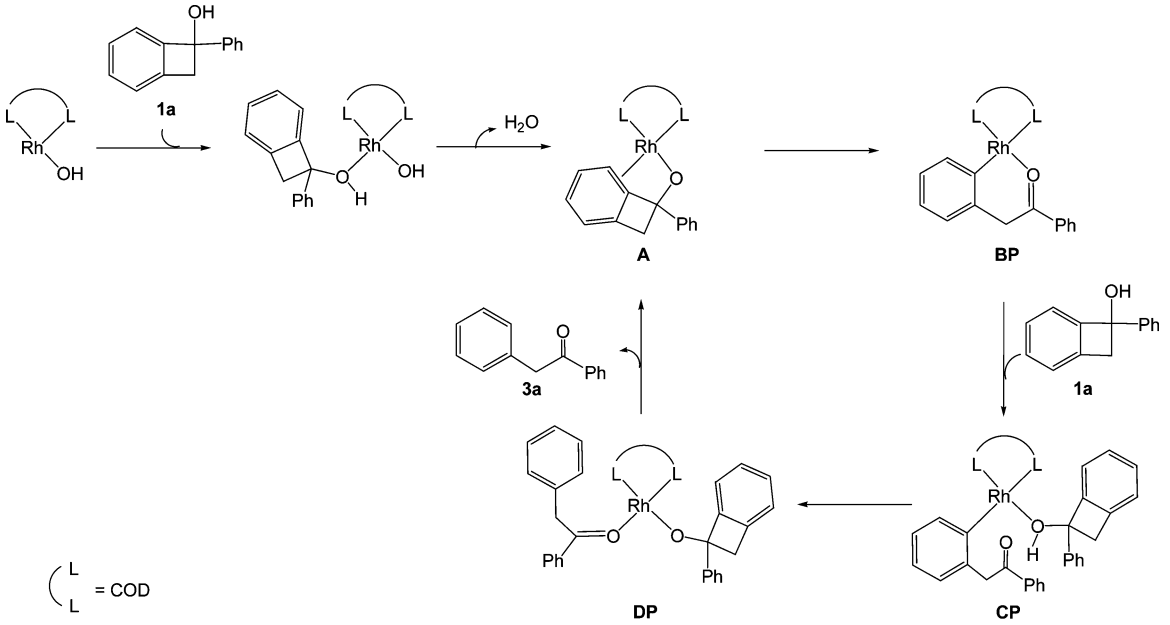

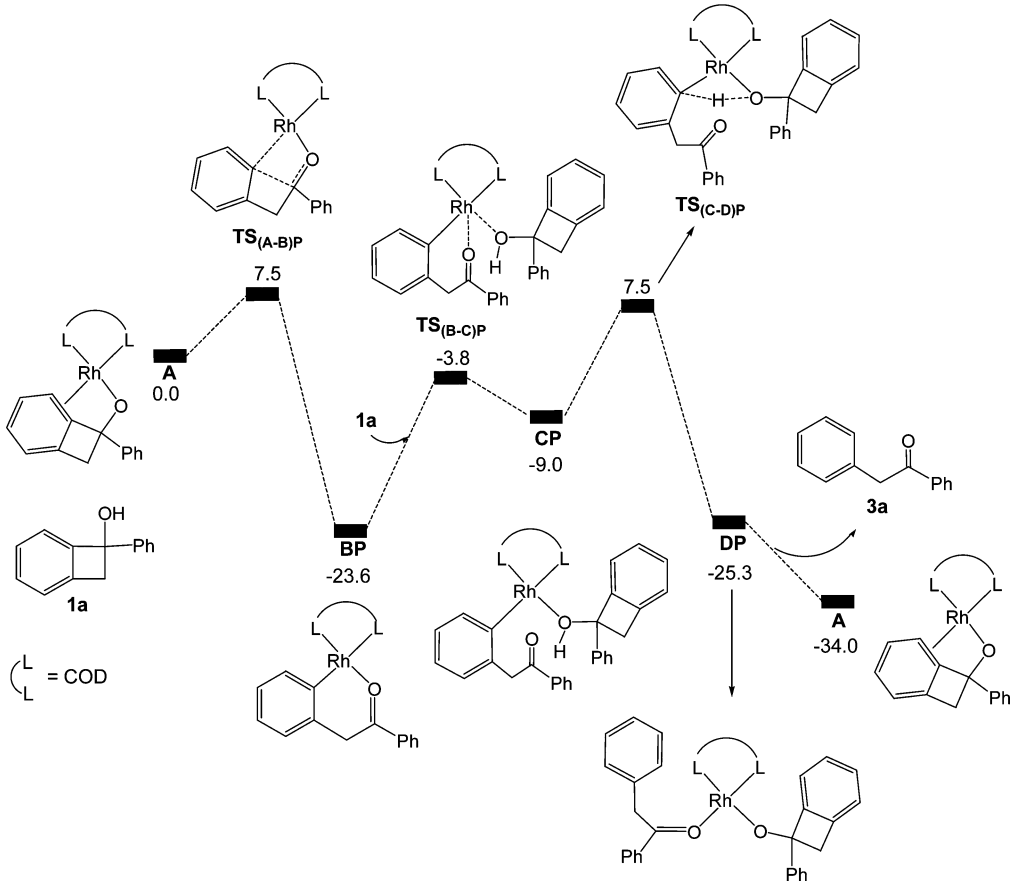

Figure 1. Free energy profile calculated for the Rh-catalyzed ring-opening reactions of phenylcyclobutabenzenol on the basis of the mechanism proposed in Scheme 1. The relative free energies are given in kcal/mol.

gives the intermediate **CP**. Subsequently, a proton migration produces the product molecule, 1,2-diphenylethanone (**3a**), as a ligand. Finally, a ligand exchange of **1a** for the coordinated phenyl moiety in **DP** releases the product molecule (1,2-diphenylethanone (**3a**)) and regenerates the active species **A**.

Despite the fact that the reaction mechanism (Scheme 1) can account for the formation for the product 1,2-diphenylethanone (**3a**) observed experimentally, detailed aspects regarding the structures and energetics of the intermediates and transition states are needed in order to understand the issue related to the

dx.doi.org/10.1021/jo4019123 | J. Org. Chem. 2013, 78, 11357−11365

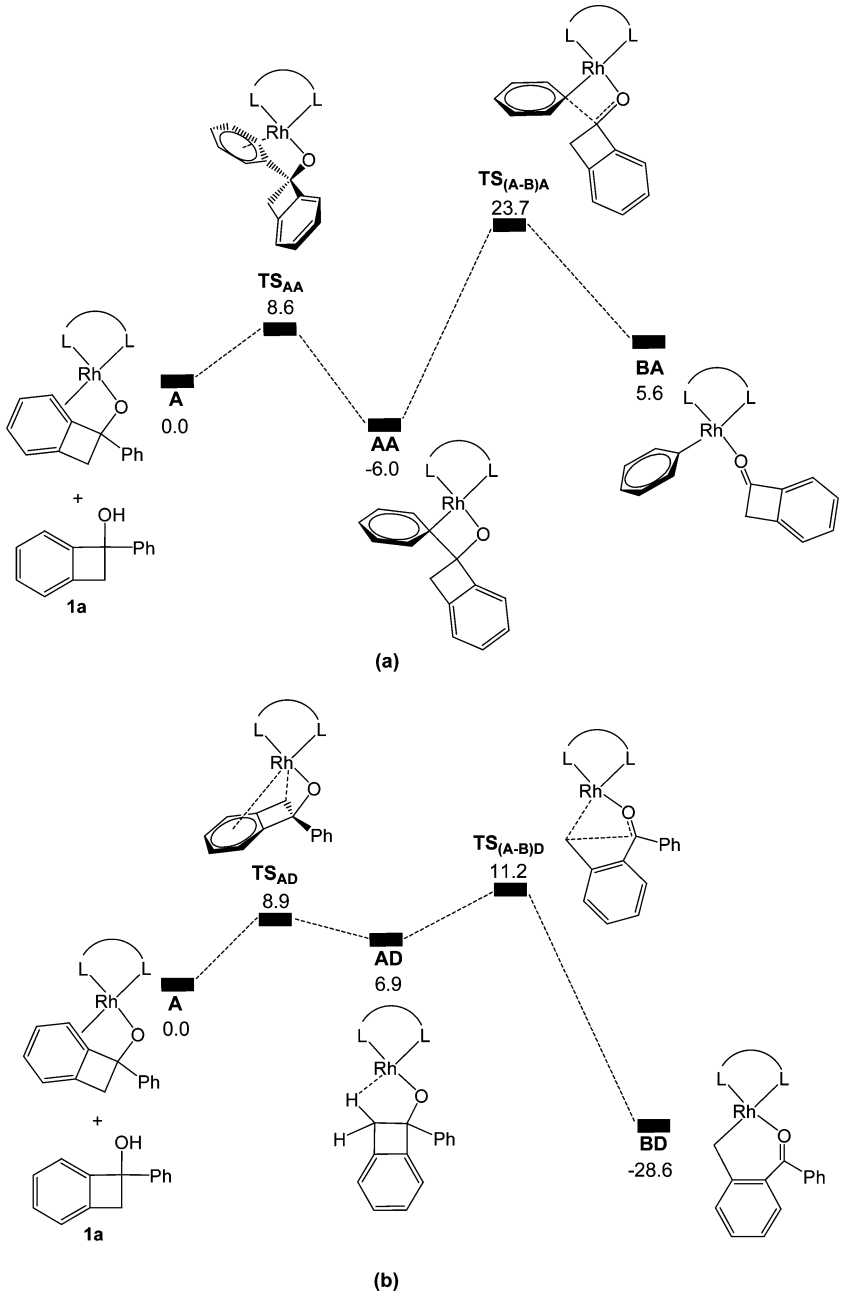

Figure 2. Free energy profiles calculated for the Rh-catalyzed β-carbon elimination involving the cleavage of (a) the unstrained C(sp^2)−C(sp^3) bond and (b) the C(sp^3)−C(sp^3) bond. The relative free energies are given in kcal/mol.

site selectivity observed and mentioned above. In this paper, with the aid of DFT calculations, we examine in detail the mechanism of the Rh-catalyzed ring-opening reactions of phenylcyclobutabenzenol (**1a**). We hope that the insight provided will be helpful for understanding the site selectivity in the ring-opening reactions. With the results obtained, we will also discuss the mechanism related to the catalyzed reactions shown in eq 3 involving insertion of alkynes into the C(sp^2)−C(sp^3)(OH)(Ph) single bond of phenylcyclobutabenzenol (**1a**).

■ COMPUTATIONAL DETAILS

Geometry optimizations have been performed at the Becke3LYP (B3LYP) level of density functional theory.[11] The effective core potentials (ECPs) of Hay and Wadt with a double-ζ valence basis set (LanL2DZ)[12] were used to describe Rh. Polarization functions were added for Rh (ζ_f = 1.35).[13] The 6-31G(d) basis set was used for all the other atoms. Frequency calculations were carried out to confirm the characteristics of all of the optimized structures as minima or transition states. Calculations of intrinsic reaction coordinates (IRC)[14] were also performed to confirm that transition states connect two relevant minima.

To obtain solvation-corrected relative free energies, we employed a continuum medium to do single-point calculations for all species studied, using UAKS radii on the conductor polarizable continuum model (CPCM).[15] Toluene was employed as the solvent (according to the reaction conditions) in the CPCM calculations. All calculations were performed with the Gaussian 09 software package.[16] Natural bond orbital (NBO) analysis was also performed at the same level of theory using the NBO 5.9 standalone package.[17]

To examine whether the aforementioned theoretical calculations give reliable results, we also performed single-point energy CPCM calculations for the structures involved in the C−C bond cleavage steps using the M06 DFT functional[18] with the 6-311++G** basis set

dx.doi.org/10.1021/jo4019123 | J. Org. Chem. 2013, 78, 11357−11365

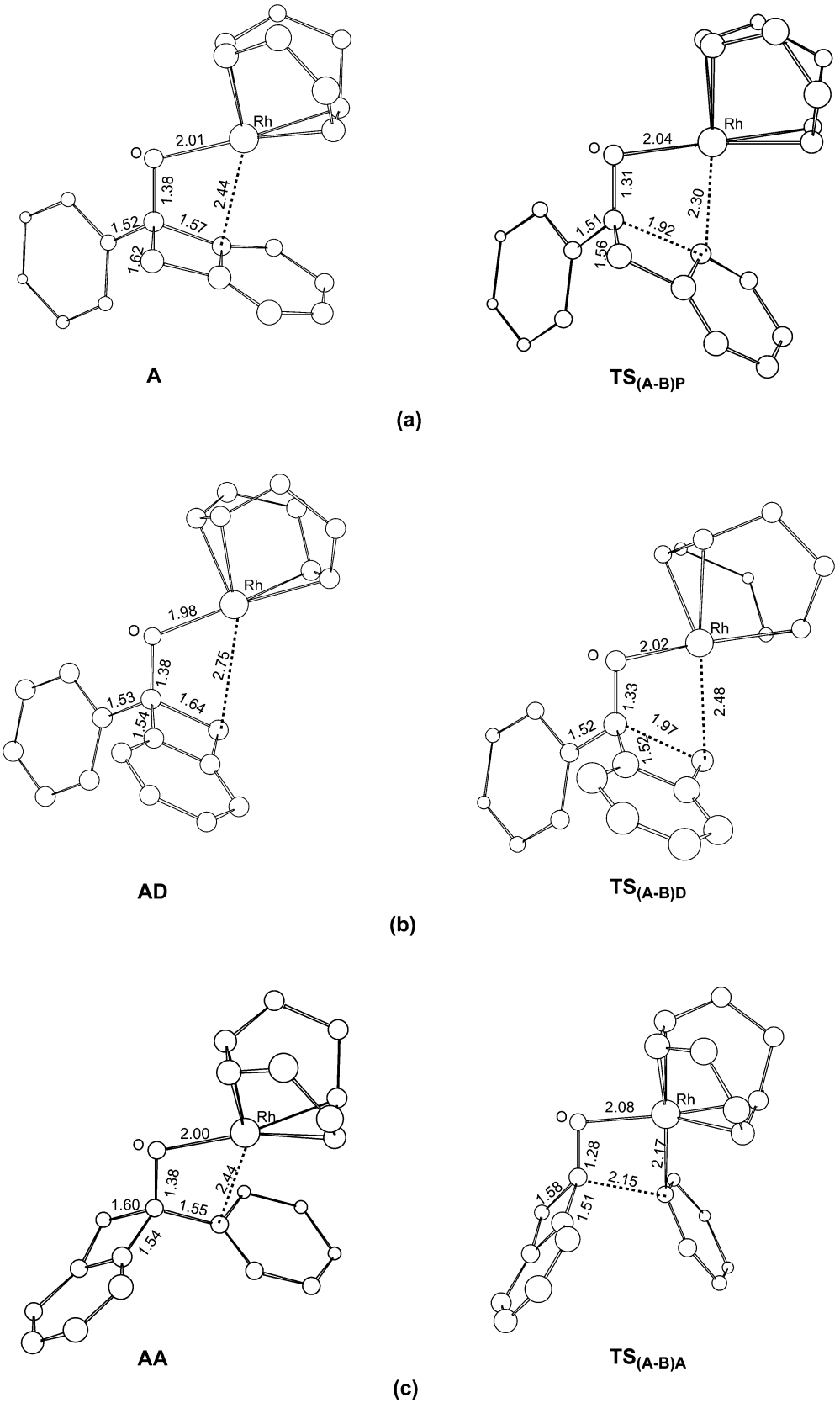

Figure 3. Selected bond distances (Å) calculated for (a) **A** and $\mathbf{TS}_{(\mathbf{A\text{-}B})\mathbf{P}}$, (b) **AD** and $\mathbf{TS}_{(\mathbf{A\text{-}B})\mathbf{D}}$, and (c) **AA** and $\mathbf{TS}_{(\mathbf{A\text{-}B})\mathbf{A}}$. Hydrogen atoms have been omitted for the purpose of clarity.

for C, H, and O and the same basis set described above for Rh. These additional calculations show that the level of theory we used is reliable for the systems studied in this work. For example, with the higher level of calculations, the free energy barriers calculated for the steps **A** → **BP** (Figure 1), **A** → **BA** (Figure 2), and **A** → **BD** (Figure 2) are 6.9, 24.0, and 12.7 kcal/mol, respectively. With the lower level of calculations, the

dx.doi.org/10.1021/jo4019123 | *J. Org. Chem.* 2013, 78, 11357−11365

corresponding barriers calculated are 7.5, 23.7, and 11.2 kcal/mol, respectively.

RESULTS AND DISCUSSION

Mechanism and Site Selectivity in the Rh-Catalyzed Ring-Opening Reactions of Phenylcyclobutabenzenol (1a). We first calculated the energy profile for the Rh-catalyzed ring-opening reactions of phenylcyclobutabenzenol (**1a**) on the basis of the mechanism proposed and shown in Scheme 1. Figure 1 shows the energy profile calculated, with **A** + **1a** being taken as the reference point. The calculated molecular geometry of the active species **A** features a square-planar structure and contains an Rh–η^2-aryl interaction. From Figure 1, we can see that the active species **A** undergoes β-carbon elimination via the transition state $\mathbf{TS}_{(\mathbf{A\text{-}B})\mathbf{P}}$, yielding the ring-opened arylrhodium **BP** with a barrier of only 7.5 kcal/mol. From the intermediate **BP**, a ligand exchange via the transition state $\mathbf{TS}_{(\mathbf{B-C})\mathbf{P}}$ gives another intermediate, **CP**. Subsequently, a proton transfer (alcoholysis) in the intermediate **CP** gives the complex **DP** via the transition states $\mathbf{TS}_{(\mathbf{C\text{-}D})\mathbf{P}}$. The rate-determining step corresponds to ligand exchange followed by alcoholysis with an overall reaction free energy barrier of 31.1 kcal/mol. Finally, from **DP**, release of the product molecule 1,2-diphenylethanone **3a** regenerates the active species **A**. The overall reaction is exergonic with a reaction free energy of −34.0 kcal/mol.

The energy profile given in Figure 1 suggests that the mechanism proposed in Scheme 1 is reasonable to account for the formation of product 1,2-diphenylethanone (**3a**). The calculated overall reaction free energy barrier (31.1 kcal/mol) is moderately high, consistent with the experimental condition that the catalytic reactions were carried out at 100 °C. The mechanism shown in Scheme 1 considers a β-carbon elimination with cleavage of a strained C(sp^2)–C(sp^3)(OH)(Ph) bond. It is understandable that cleavage of the unstrained C(sp^2)–C(sp^3) bond in **1a** involving β-phenyl elimination does not occur when the relative bond strengths of the two bonds mentioned are considered.[19] However, it is interesting that a β-carbon elimination involving cleavage of the C(sp^3)–C(sp^3) bond in the four-membered ring does not occur, even though the C(sp^3)–C(sp^3) bond is considerably weak in comparison to the other two C(sp^2)–C(sp^3) bonds mentioned above.

In order to obtain further insight into the C–C bond selective cleavage, we calculated and compared the energy profiles for the β-carbon elimination steps involving the cleavage of the unstrained C(sp^2)–C(sp^3) bond and the C(sp^3)–C(sp^3) bond in **1a** (Figure 2). Starting from the active species **A**, isomerization through rotation of the aryl group around the C–O single bond can give both the intermediates **AA** (Figure 2a) and **AD** (Figure 2b). The intermediate **AA** contains an Rh–η^2-phenyl interaction and is 6.0 kcal/mol more stable than **A**, while the intermediate **AD** contains an agostic interaction and is 6.9 kcal/mol less stable than **A**. Figure 2 shows that the transition states for the β-phenyl elimination involving cleavage of the unstrained C(sp^2)–C(sp^3) bond has a higher barrier than that of the β-carbon elimination involving cleavage of the C(sp^3)–C(sp^3) bond. The calculated energy profiles given in Figures 1 and 2 show that the β-carbon elimination involving cleavage of the strained C(sp^2)–C(sp^3)(OH)(Ph) bond, giving the product molecule of 1,2-diphenylethanone (**3a**) observed experimentally, is most favored.

Figure 3 gives the optimized structures, together with selected bond distances, for the intermediates and the transition states involved in the β-carbon elimination steps shown in Figures 1 and 2. In the most favorable β-carbon elimination transition state structure $\mathbf{TS}_{(\mathbf{A\text{-}B})\mathbf{P}}$ (Figure 3a), the orientation of the phenyl ring involved in the β-carbon elimination allows both the σ and π orbitals centered at the migrating ipso carbon to simultaneously interact with the metal center and the carbonyl carbon of the substrate ligand.[20] Clearly, the available π system involved in the β-carbon elimination facilitates the elimination process.

In the β-phenyl elimination transition state $\mathbf{TS}_{(\mathbf{A\text{-}B})\mathbf{A}}$ (Figure 3c), an available π system is also involved. However, the cleaved C(sp^2)–C(sp^3) bond is relatively stronger. In the β-carbon elimination transition state $\mathbf{TS}_{(\mathbf{A\text{-}B})\mathbf{D}}$ (Figure 3b), which involves cleavage of the strained the C(sp^3)–C(sp^3) bond, such a π system is not available, making the elimination barrier relatively higher.

Thermal Cleavage of the Three C–C σ Bonds in the Four-Membered Ring of 1a. As mentioned in the Introduction, simple heating of phenylcyclobutabenzenol (**1a**) in toluene at 100 °C

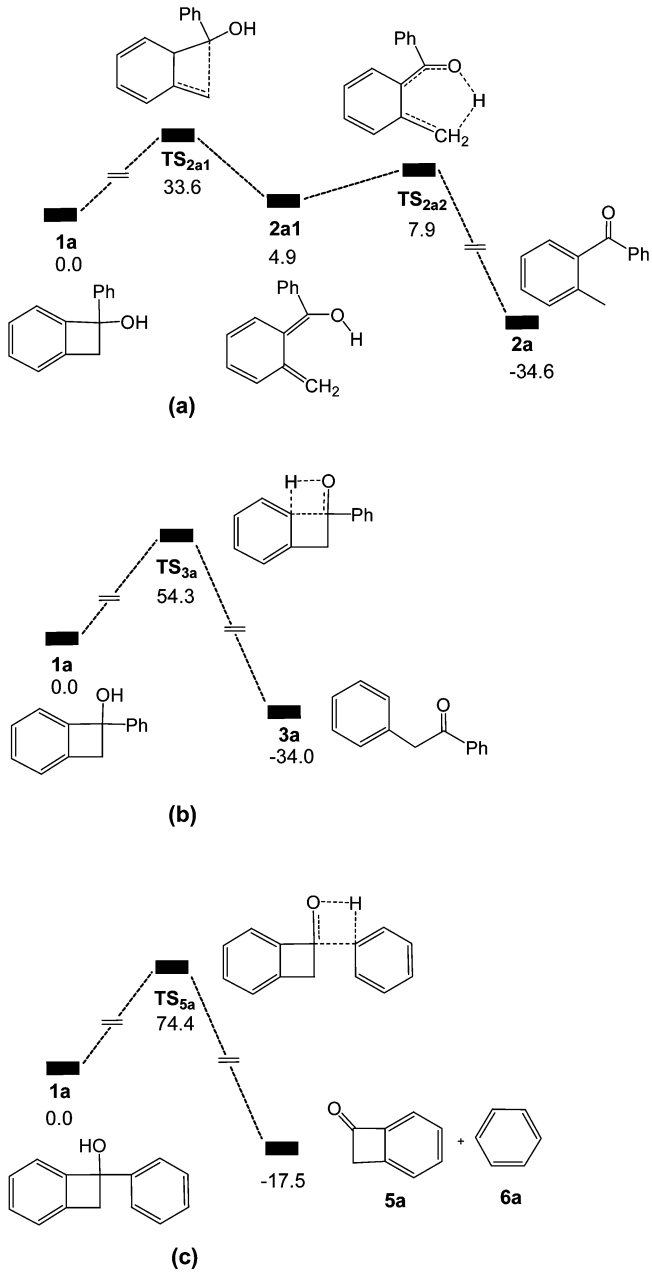

Figure 4. Free energy profile calculated for the thermal cleavage of (a) the C(sp^3)–C(sp^3) bond, (b) the strained C(sp^2)–C(sp^3)(OH)(Ph) bond, and (c) the unstrained C(sp^2)–C(sp^3) bond. The relative free energies are given in kcal/mol.

dx.doi.org/10.1021/jo4019123 | J. Org. Chem. 2013, 78, 11357–11365

Scheme 2

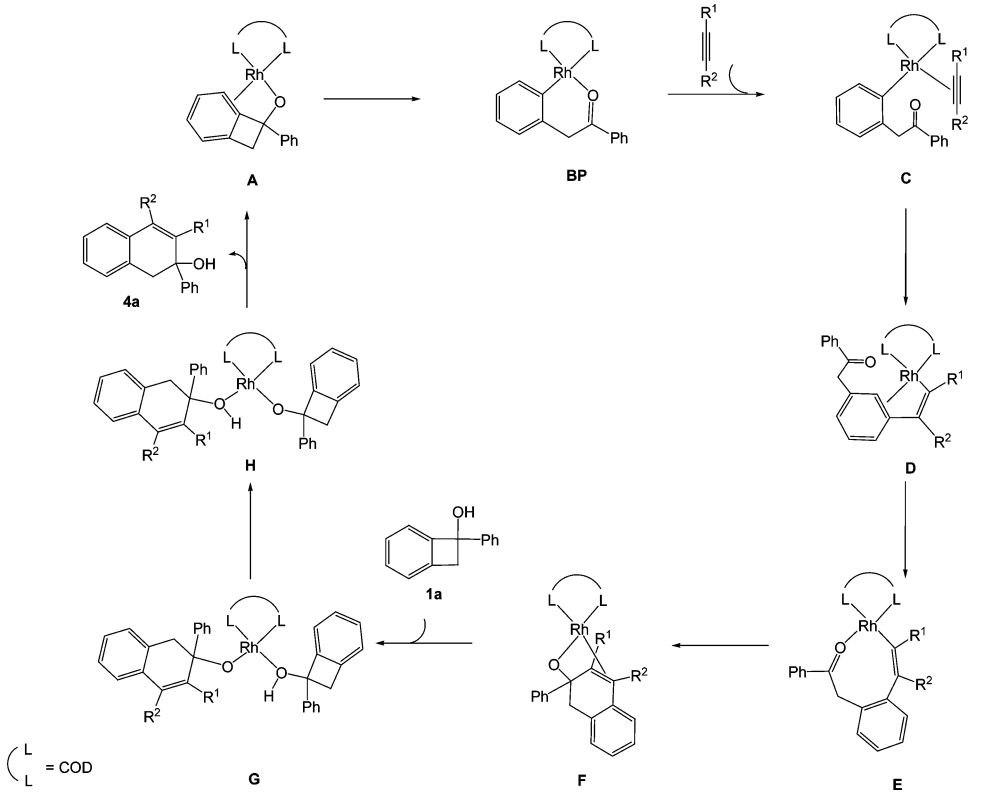

selectively cleaved the C(sp^3)−C(sp^3) single bond and gave 2-methylbenzophenone (**2a**) in high yield (eq 1). To investigate the energetic aspect associated with the experimental observation, we calculated the energy profile for the thermal cleavage of the C(sp^3)−C(sp^3) bond. Figure 4a shows that the transformation of **1a** to **2a** consists of two steps. In the first step, the C(sp^3)−C(sp^3) bond cleavage gives a dearomatized species. In the second step, a proton migration affords the thermal cleavage product **2a**. The overall free energy barrier is 33.6 kcal/mol.

For comparison, we also investigated the energetic aspect for the thermal cleavage of the other two C−C bonds involving the carbon atom to which the alcohol group is attached. Figure 4b,c shows the energy profiles calculated. The barriers (54.3 and 74.4 kcal/mol) were calculated to be inaccessibly high.

Summarizing all these results, we can understand that, in the absence of the rhodium catalyst, only the reaction shown in eq 1 can be observed, which has a rate-determining free energy barrier of 33.6 kcal/mol (Figure 4a). In the presence of the rhodium catalyst, the reaction shown in eq 2 was observed, which has a rate-determining free energy barrier of 31.1 kcal/mol (Figure 1).

Mechanism and Regioselectivity in the Rh-Catalyzed Insertion Reactions of Alkynes with Phenylcyclobutabenzenol (1a). As mentioned in the Introduction, we will also study the mechanism related to the catalyzed reactions shown in eq 3 involving insertion of alkynes into the C(sp^2)−C(sp^3)-(OH)(Ph) single bond of phenylcyclobutabenzenol (**1a**). The mechanism shown in Scheme 2 was proposed by Murakami et al. to account for the reactions, which includes eight major steps. (i) β-Carbon elimination cleaves the strained C(sp^2)−C(sp^3)(OH)-(Ph) single bond of **1a** to give the intermediate **BP**. This step is the same as that shown in Scheme 1. (ii) A ligand exchange of an alkyne molecule for the coordinated C═O moiety gives the intermediate **C**. (iii) Insertion of alkyne into the Rh−C(sp^2) bond in **C** gives the intermediate **D**, in which an Rh−η^2-aryl bonding interaction is present. (iv) Rearrangement of the intermediate **D** gives the eight-membered-ring metallacycle **E**. In the metallacycle **E**, the C═O moiety is coordinated to the metal center. (v) Insertion of the C═O moiety into the Rh−C(sp^2) bond in **E** gives the intermediate **F**. In the intermediate **F**, the C═C moiety originally from the alkyne molecule is coordinated to the metal center in an η^2 fashion. (vi) From **F**, a ligand exchange of **1a** for the coordinated C═C moiety gives the intermediate **G**. (vii) A proton migration in the intermediate **G** gives the intermediate **H**, in which the product molecule **4a** acts as a ligand. (viii) Finally, dissociation of the product molecule **4a** regenerates the active species **A**.

In eq 3 when asymmetric alkynes are used, regioisomeric products are possible. Experimentally, high regioselectivity was also observed. For example, the Rh-catalyzed alkyne insertion reaction of MeC≡CPh with phenylcyclobutabenzenol (**1a**) gives the product **7a** (eq 4). To understand the interesting regioselectivity observed, we calculated the energy profiles for the reaction shown in eq 4 on the basis of the proposed mechanism shown in Scheme 2.

Figure 5 shows the energy profiles calculated for the Rh-catalyzed alkyne insertion reaction of MeC≡CPh with phenylcyclobutabenzenol (**1a**) (eq 4) on the basis of the mechanism proposed in Scheme 2. The first step is the same as that shown in Figure 1, which is the β-carbon elimination in **A** via the transition state $\mathbf{TS}_{(\mathbf{A\text{-}B})\mathbf{P}}$ giving the ring-opened arylrhodium **BP**. From the intermediate **BP**, a ligand exchange of an alkyne molecule (phenyl−methylacetylene) for the coordinated C═O moiety gives the intermediate **C** followed by insertion of the asymmetric alkyne into the Rh−C(sp^2) bond in the intermediate **C**.

Considering the relative orientation of the coordinated asymmetric alkyne, two pathways for the alkyne insertion are

dx.doi.org/10.1021/jo4019123 | J. Org. Chem. 2013, 78, 11357−11365

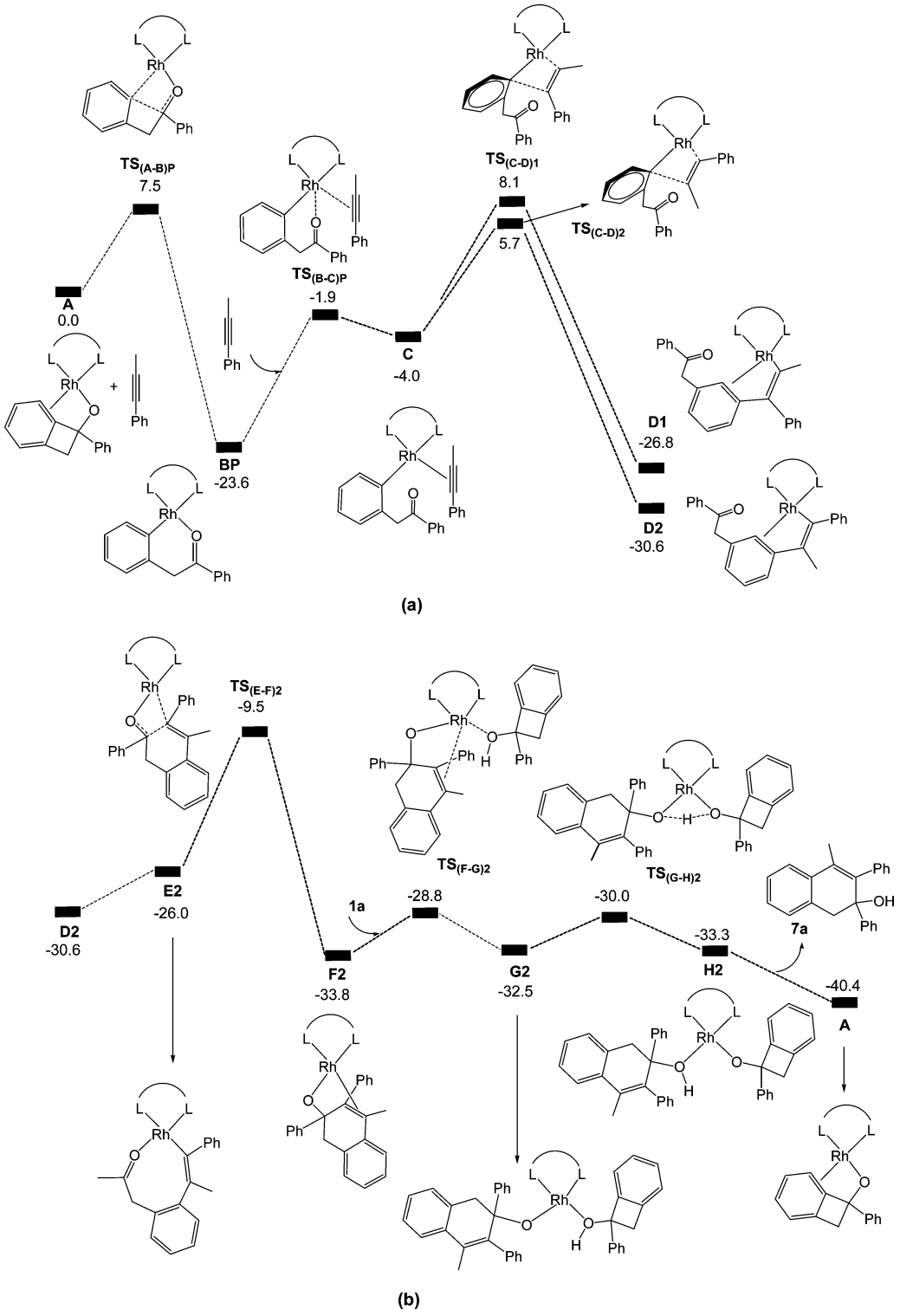

Figure 5. Free energy profile calculated for the Rh-catalyzed alkyne insertion reaction of MeC≡CPh with phenylcyclobutabenzenol (**1a**) on the basis of the mechanism proposed in Scheme 2: (a) step **A** → **D** shown in Scheme 2; (b) step **D** → **A** shown in Scheme 2. The relative free energies are given in kcal/mol.

possible. Figure 5a shows that the pathway leading to formation of **D2**, in which the metal-bonded carbon in **C** forms a bond with the methyl-substituted carbon of MeC≡CPh, is more favorable than that leading to formation of **D1**, in which the metal-bonded carbon in **C** forms a bond with the phenyl-substituted carbon of MeC≡CPh. The overall barrier for the favorable alkyne insertion pathway was calculated to be 29.3 kcal/mol, corresponding to the energy difference between **BP** and $\mathbf{TS}_{(C\text{-}D)2}$. In fact, this overall barrier is also the rate-determining barrier for the whole catalytic cycle. The experimentally observed regioselectivity was also closely related to this alkyne insertion step.

It is known that insertion of an alkyne or alkene ligand into a metal−C σ bond mainly involves an orbital interaction of the occupied M−C σ bonding orbital with an unoccupied π^* orbital

dx.doi.org/10.1021/jo4019123 | J. Org. Chem. 2013, 78, 11357−11365

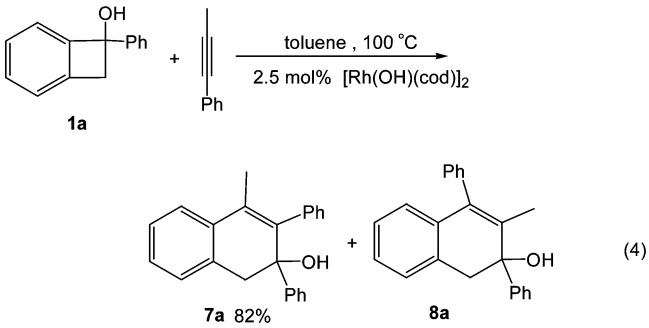

(4)

of the alkyne or alkene ligand, implying a nucleophilic attack of the M−C(sp^3) bond at either the alkyne or alkene carbon.[21] Therefore, the π-accepting Ph substituent makes the methyl-substituted carbon of MeC≡CPh π electron poorer in comparison with the Ph-substituted carbon, facilitating the coupling between the methyl-substituted carbon of MeC≡CPh and the metal-bonded carbon and leading favorably to formation of the intermediate **D2**. To substantiate our argument here, we performed NBO calculations for the intermediate **C** and indeed found that the Ph-substituted carbon in the coordinated MeC≡CPh has a higher π electron density than the methyl-substituted carbon (52% versus 48%).

From the relative stability of **BP** and **D2** together with the barrier heights in the steps followed, we conclude that the alkyne insertion is an irreversible process. Therefore, the energy profile from **D2** forward is important (Figure 5b). From the intermediate **D2**, a rearrangement of the carbon ligand gives **E2**, in which the C═O moiety is coordinated with the metal center. Then, insertion of the C═O moiety into the Rh−C(sp^2) bond in **E2** occurs to give the intermediate **F2**, having an η^2-olefin coordination. The barrier for the whole C═O insertion step was calculated to be 21.1 kcal/mol. From **F2**, a ligand exchange of **1a** for the coordinated C═C moiety followed by a proton transfer gives the intermediate **H2** via **G2**. Finally, release of the product molecule from **H2** and recoordination of the phenyl ring to the metal center regenerate the active species **A** and complete the catalytic cycle.

Ring Opening versus Alkyne Insertion in the Rh-Catalyzed Reactions. In both the ring-opening and alkyne insertion reactions, the first step involves β-carbon elimination to give the intermediate **BP**. In the presence of an alkyne substrate, the reaction can proceed by reacting **BP** either with phenylcyclobutabenzenol (**1a**) (alcoholysis) to give the ring-opening product or with alkyne (insertion) to give the insertion product. Comparing the profiles in Figures 1 and 5a, we see that the former has a higher overall reaction barrier than the latter. These results are consistent with the experimental observation that in the presence of an alkyne substrate the insertion occurs in the Rh-catalyzed reaction.

CONCLUSIONS

The site selectivity of Rh-catalyzed ring-opening reactions of phenylcyclobutabenzenol (**1a**) has been investigated with the aid of DFT calculations. The results of the calculations supported that the mechanism involves β-carbon elimination in a rhodium(I) phenylcyclobutabenzenolato complex followed by alcoholysis. The site selectivity in the ring-opening reaction was determined in the β-carbon elimination step. In the three possible β-carbon eliminations involving the three carbons bonded to the β-carbon in the rhodium(I) phenylcyclobutabenzenolato complex, the cleavage of the strained C(sp^2)−C(sp^3) bond was kinetically most favorable in comparison with those of the C(sp^3)−C(sp^3) bond in the four-membered ring and of the unstrained C(sp^2)−C(sp^3) bond. The available π system involved in the most favorable β-carbon elimination facilitates the elimination process. In the β-phenyl elimination involving cleavage of the unstrained C(sp^2)−C(sp^3) bond, a π system is also available. However, the cleaved C(sp^2)−C(sp^3) bond is much stronger.

The energetic aspects for the thermal cleavage of the aforementioned three C−C σ bonds in the absence of the rhodium catalyst have also been computationally investigated and compared. The computational results indicate that the C(sp^3)−C(sp^3) bond in the four-membered ring of **1a**, which is the weakest among the three studied C−C σ bonds, is cleaved most easily.

We have also investigated the Rh-catalyzed insertion of the asymmetric alkyne MeC≡CPh into the C(sp^2)−C(sp^3)(OH)-(Ph) single bond of phenylcyclobutabenzenol (**1a**). The related regioselectivity issue of this reaction has also been examined. The calculation results indicate that the regioselectivity is determined in the step of alkyne insertion into the Rh−C σ bond in the intermediate generated from the most favorable β-carbon elimination in the rhodium(I) phenylcyclobutabenzenolato complex mentioned above. It was found that the π-accepting Ph substituent makes the methyl-substituted carbon of MeC≡CPh π electron poorer in comparison with the Ph-substituted carbon, facilitating the interaction between the Rh−C σ bond and the methyl-substituted carbon of MeC≡CPh during the insertion process, and eventually leading to formation of the experimentally observed regioisomer **7a**.

ASSOCIATED CONTENT

Supporting Information

Text giving the complete ref 16 and tables giving the Cartesian coordinates and electronic energies for all of the calculated structures. This material is available free of charge via the Internet at http://pubs.acs.org.

AUTHOR INFORMATION

Corresponding Author

*E-mail for Z.L.: chzlin@ust.hk.

Notes

The authors declare no competing financial interest.

ACKNOWLEDGMENTS

This work was supported by the Research Grants Council of Hong Kong (HKUST603711, HKUST603313 and CUHK7/CRF/12G).

REFERENCES

(1) (a) Ruhland, K. *Eur. J. Org. Chem.* **2012**, 2683. (b) Seiser, T.; Saget, T.; Tran, D. N.; Cramer, N. *Angew. Chem., Int. Ed.* **2011**, *50*, 7740. (c) Murakami, M.; Matsuda, T. *Chem. Commun.* **2011**, *47*, 1100. (d) Park, Y. J.; Park, J.-W.; Jun, C. *Acc. Chem. Res.* **2008**, *41*, 222.

(2) Hang, X.; Chen, Q.; Xiao, J. *J. Org. Chem.* **2008**, *73*, 8598.

(3) (a) Park, S.; Cha, J. K. *Org. Lett.* **2000**, *2*, 147. (b) Ethirajan, M.; Oh, H.; Cha, J. K. *Org. Lett.* **2007**, *9*, 2693. (c) Nishimura, T.; Ohe, K.; Uemura, S. *J. Am. Chem. Soc.* **1999**, *121*, 2645.

(4) (a) Ogata, K.; Shimada, D.; Furuya, S.; Fukuzawa, S. *Org. Lett.* **2013**, *15*, 1182. (b) Sumida, Y.; Yorimitsu, H.; Oshima, K. *Org. Lett.* **2010**, *12*, 2254.

(5) Ghorai, M. K.; Shukla, D.; Bhattacharyya, A. *J. Org. Chem.* **2012**, *77*, 3740.

(6) Iwata, A.; Inuki, S.; Oishi, S.; Fujii, N.; Ohno, H. *J. Org. Chem.* **2011**, *76*, 5506.

(7) Venkatasubbaiah, K.; Zhu, X.; Kays, E.; Hardcastle, K. I.; Jones, C. W. *ACS Catal.* **2011**, *1*, 489.
(8) (a) Sawama, Y.; Sawama, Y.; Krause, N. *Org. Lett.* **2009**, *11*, 5034. (b) Shi, M.; Liu, L.; Tang, J. *Org. Lett.* **2006**, *8*, 4043.
(9) (a) Elsässer, B.; Schoenen, I.; Fels, G. *ACS Catal.* **2013**, *3*, 1397. (b) Schalk, O.; Broman, S. L.; Petersen, M. Å.; Khakhulin, D. V.; Brogaard, R. Y.; Nielsen, M. B.; Boguslavskiy, A. E.; Stolow, A.; Sølling, T. I. *J. Phys. Chem. A* **2013**, *117*, 3340. (c) Zhao, Z.; Moskaleva, L. V.; Rösch, N. *ACS Catal.* **2013**, *3*, 196.
(10) Ishida, M.; Sawano, S.; Masuda, Y.; Murakami, M. *J. Am. Chem. Soc.* **2012**, *134*, 17502.
(11) (a) Becke, A. D. *J. Chem. Phys.* **1993**, *98*, 5648. (b) Miehlich, B.; Savin, A.; Stoll, H.; Preuss, H. *Chem. Phys. Lett.* **1989**, *157*, 200. (c) Lee, C.; Yang, W.; Parr, G. *Phys. Rev. B* **1988**, *37*, 785. (d) Stephens, P. J.; Devlin, F. J.; Chaobalowski, C. F. *J. Phys. Chem.* **1994**, *98*, 11623.
(12) (a) Wadt, W. R.; Hay, P. J. *J. Chem. Phys.* **1985**, *82*, 284. (b) Hays, P. J.; Wadt, W. R. *J. Chem. Phys.* **1985**, *82*, 299.
(13) (a) Ehlers, A. W.; Böhme, M.; Dapprich, S.; Gobbi, A.; Höllwarth, A.; Jonas, V.; Köhler, K. F.; Stegmenn, R.; Frenking, G. *Chem. Phys. Lett.* **1993**, *208*, 111. (b) Höllwarth, A.; Böhme, M.; Dapprich, S.; Ehlers, A. W.; Gobbi, A.; Jonas, V.; Köhler, K. F.; Stegmenn, R.; Veldkamp, A.; Frenking, G. *Chem. Phys. Lett.* **1993**, *208*, 237.
(14) (a) Fukui, K. *J. Phys. Chem.* **1970**, *74*, 4161. (b) Fukui, K. *Acc. Chem. Res.* **1981**, *14*, 363.
(15) (a) Cossi, M.; Rega, N.; Scalmani, G.; Barone, V. *J. Comput. Chem.* **2003**, *24*, 669. (b) Cossi, M.; Barone, V.; Cammi, R.; Tomasi, J. *Chem. Phys. Lett.* **1966**, *255*, 327. (c) Cossi, M.; Barone, V.; Mennucci, B.; Tomasi, J. *Chem. Phys. Lett.* **1988**, *286*, 253. (d) Cossi, M.; Barone, V.; Robb, M. A. *J. Chem. Phys.* **1999**, *111*, 5295.
(16) Frisch, M. J.; et al. *Gaussian 09, revision D.01*; Gaussian, Inc., Pittsburgh, PA, 2009.
(17) (a) Reed, A. E.; Weinstock, R. B.; Weinhold, F. *J. Chem. Phys.* **1985**, *83*, 735. (b) Glendening, E. D.; Badenhoop, J. K.; Reed, A. E.; Carpenter, J. E.; Bohmann, J. A.; Morales, C. M.; Weinhold, F. *NBO 5.9*; Theoretical Chemistry Institute, University of Wisconsin: Madison, WI, 2011.
(18) (a) Zhao, Y.; Truhlar, D. G. *Acc. Chem. Res.* **2008**, *41*, 157. (b) Zhao, Y.; Truhlar, D. *Theor. Chim. Acta* **2008**, *120*, 215.
(19) (a) Seiser, T.; Saget, T.; Tran, D. N.; Cramer, N. *Angew. Chem., Int. Ed.* **2011**, *50*, 7740. (b) Bach, R. D.; Dmitrenko, O. *J. Am. Chem. Soc.* **2004**, *126*, 4444.
(20) Xue, L.; Ng, K, N.; Lin, Z. *Dalton Trans.* **2009**, 5841.
(21) (a) Margl, P.; Deng, L.; Ziegler, T. *J. Am. Chem. Soc.* **1998**, *120*, 5517. (b) Niu, S.; Hall, M. B. *Chem. Rev.* **2000**, *100*, 353. (c) Bai, T.; Zhu, J.; Xue, P.; Sung, H. H.-Y.; Williams, I. D.; Ma, S.; Lin, Z.; Jia, G. *Organometallics* **2007**, *26*, 5581. (d) Li, Y.; Lin, Z. *Organometallics* **2013**, *32*, 3003.